



PREPARATION AND CHARACTERIZATION OF NANOSTRUCTURED LIPID CARRIERS OF ANTINEOPLASTIC AGENTS

Amrendra Pratap Yadav, Mohan Lal Kori*

Vedica College of B. Pharmacy, Bhopal, Madhya Pradesh, India

*Corresponding author: mlkori.research@gmail.com

ABSTRACT

The aim of this study was to prepare and characterize folic acid conjugated nanostructure lipid carriers (NLCs) as nanocarriers for parenteral delivery of gemcitabine (GEM) and paclitaxel (PTX). Folic acid-conjugated GEM-PTX-NLCs were prepared by solvent emulsion-evaporation method and characterized for particle size, polydispersity index and zeta potential which were found to be 134.62 ± 4.11 nm, 0.189 ± 0.05 , $+28.4 \pm 0.6$ mV, respectively. Percent entrapment efficiency of GEM and PTX in FA-conjugated GEM-PTX- NLCs were recorded as 89.1 ± 0.6 % and 86.6 ± 0.8 % respectively, which was within an acceptable range for injectable formulation. *In vitro* drug release study of optimized formulation was carried out using the dialysis tube method. FA-conjugated GEM-PTX-loaded NLCs showed cumulative drug release 78.6 ± 0.93 % and 75.3 ± 0.7 % of GEM and PTX respectively in 72 h in PBS pH 7.4: methanol (7:3) while FA-conjugated GEM-PTX- NLCs showed cumulative drug release 85.5 ± 0.075 % and 82.2 ± 0.72 % of GEM and PTX respectively in 72 h in PBS pH 4.0 : methanol (7:3). Furthermore, stability testing data indicated that NLCs formulations stored at $5^\circ\text{C} \pm 3^\circ\text{C}$ were more stable than those stored at $25^\circ\text{C} \pm 2^\circ\text{C}/60\% \text{ RH} \pm 5\% \text{ RH}$. These results suggest that folic acid-conjugated GEM-PTX- NLCs have the potential for serving as a novel carrier system for delivery of antineoplastic agents.

Keywords: Nanostructured lipid carrier, Antineoplastic agent, Paclitaxel, Gemcitabine.

1. INTRODUCTION

Lipid nanoparticles such as nanostructured lipid carriers (NLCs) have been put forward as established and alternative colloidal drug carrier systems [1, 2]. Nanostructured lipid carriers are a new type of delivery system offering improved performance in terms of drug loading and long term stability with the ability to form highly concentrated dispersions. A new generation of nanostructured lipid carriers (NLCs) consisting of a lipid matrix with a special nanostructure has been developed [3]. NLCs were primarily considered for the delivery of lipophilic drugs but their suitability for hydrophilic drugs is now well established. Biocompatible nature of lipids is responsible for its development as a promising drug delivery [4]. Folic acid (FA) ligand has a high affinity toward Folate receptor (FR), and facilitates specific binding to FR on the surface of various cancerous cells. Hence, the FA ligand is a versatile moiety on the surface of vehicles to provide an efficient FR-mediated endocytosis and targeted delivery of drug to tumor tissue [5]. In chemotherapy, the most common classes of drugs include alkylates to inhibit DNA transcription,

antimetabolites - cellular compound analogs - that block metabolic pathways in the S-phase, microtubule-stabilizing agents in the G0/G1 and/or G2/M phases, and topoisomerase inhibitors. Gemcitabine (GEM) is an antimetabolite drug used to treat many cancers as it interferes in DNA replication, inhibiting deoxyribonucleotide synthesis in the S-phase which leads to anticancer effects during cell division. In the late phases, cancer cells are highly resistant to chemotherapy and to improve treatment efficiency, researchers are keen to the simultaneous application of different drugs, such as the combination of GEM with taxol, capecitabine, cisplatin and oxaliplatin. Nevertheless, only therapies using GEM+Taxol demonstrated affect better than single therapy with GEM in clinical trials. Combined administration of GEM and paclitaxel (PTX) increases the survival rate by at least two months in patients with metastases, being considered a novel therapeutic procedure for cancer [6].

Amazingly little has been known for many years about the prevailing mechanisms the emulsion-solvent evaporation process. The main physical processes are

quite simple: a polymer is dissolved in a decent solvent, which is then emulsified in an aqueous medium containing a surfactant. The slow evaporation of the polymer solvent pointed to nucleation of the polymer on the water-solvent interface. After evaporation of the solvent, the dispersions can be dialyzed to remove unwanted or low molecular weight polymers and can be freeze-dried [7].

Drug Loaded NLCs were characterized for, a) particle size and morphology: the size of the particles affects their surface area and hence their solubility and biocompatibility as well as the rate of drug release. However, site-specific NLCs, especially those suggested as carriers for chemotherapeutic agents, should have a diameter range of 50-300 nm for increased cellular uptake [8], b) Surface Charge: A greater surface charge is accompanied with an increase in electrostatic repulsion and less aggregation between the particles. Generally, stable NLCs should have a minimum ZP of ± 20 mV [9], c) Encapsulation Efficiency Percentage: EE % significantly affects the release of the drug from NLCs as higher encapsulation alters the concentration gradient and rate of drug release. EE % values more than 60% usually indicate the success of the preparation method in loading a proper amount of the drug in the lipid particles [10], d) Storage temperature affects the stability of drug-loaded NLCs. drug-loaded NLCs were stable at low temperature (4°C) for 28 days, while higher temperatures of 25°C for 72h resulted in the occurrence of particle aggregation and decrease in surface charge. This is due to breakage of the hydrogen bonds between the surfactant molecules at the lipid/water interface as a result of increasing temperature [11].

2. MATERIAL AND METHODS

2.1. Material

Soybean Phosphatidylcholine and 1, 2-Distearoyl Phosphatidylethanolamine (DSPE). Folic acid (FA), Stearic acid, N-hydroxysuccinimide (NHS), dicyclohexylcarbodiimide (DCC), 1-ethyl-3-(3-dimethylamino-propyl) carbodiimide (EDC) and cetyltrimethylammonium bromide (Cetrimide) were purchased from Sigma Aldrich, USA. All other chemicals and reagents used were analytical grade.

2.2. Synthesis of Folate-DSPE Conjugates

Folate-DSPE was synthesized in two steps: step I involved the synthesis of NHS-ester of folic acid which was subsequently conjugated to activate DSPE in step II. In Step I Synthesis of N-hydroxysuccinimide of folic acid

(NHS-folate) was performed according to method reported by Lee *et al.* [12]. Briefly, folic acid (1 g) was dissolved in 20 ml of DMSO and 0.5 ml of TEA. Then, 0.94 g of DCC was accurately weighed and added to the solution and stirred for 1 h at room temperature under dark condition. Subsequently, 0.52 g of NHS was added to the mixture that was again stirred overnight under the same conditions. The byproduct dicyclohexyl urea (DCU) was removed by using centrifugation followed by filtration. The DMSO solution was then concentrated under reduced pressure, and the NHS-folate conjugate obtained was washed several times with anhydrous ether, dried under vacuum, and stored as yellow powder. Step II consisted of coupling of carboxyl end of NHS-ester of folic acid with amine group of DSPE. The folic acid was covalently coupled through its carboxyl group to the amino group of DSPE using EDC as a coupling agent. An equimolar amount of the above synthesized N-hydroxysuccinimide ester of folic acid and DSPE was dissolved in a common solvent. EDC was added to the folic acid DSPE solution and stirred continuously for 4 h at room temperature. Excessive amount of folic acid was removed by dialysis using a membrane with MW 2000 Da cut off and stored at 4°C. Conjugation was confirmed by using IR spectroscopy and ¹H NMR spectroscopy.

2.3. Preparation of Nanostructured lipid carrier

For the preparation of nanostructured lipid carriers, solvent emulsion-evaporation method reported by Di *et al.* [13] was used with slight modification. By this method, nanostructured lipid carriers (NLCs) can be prepared by rapidly injecting a solution of lipid and stearic acid in organic solvent into water. Briefly, 200 mg of GEM was dissolved in 10 ml water and then stirred with 1ml of triethylamine (TEA) in 3ml of acetone overnight to obtain the GEM base. FA-conjugated-DSPE (10%) was added as a co-lipid with soybean phosphatidylcholine lipid (500 mg), Stearic acid (500 mg) and Paclitaxel (100 mg) were mixed and dissolved into a mixture of acetone (5 ml) and ethanol (5 ml) in a water bath at 70°C to obtain lipid phase. At the same time, GEM HCl base was added into an aqueous Cetrimide solution (100 ml, containing 0.5% Cetrimide) and heated to the same temperature. The lipid phase was then injected into a hot surfactant solution using a mechanical agitate (1000 rpm, 1h). The NLCs dispersed warm o/w nanoemulsion into icy distilled water (0°C). By using the same method as mentioned above, the paclitaxel-gemcitabine nanostructured lipid carrier(s) were

prepared by using plane DSPE as a co-lipid with soybean phosphatidylcholine.

2.4. Design of experiment

Initial screening trials were carried out for evaluation of the formulation and processing aspects of nanocarrier. Various factors like content of lipids (250 to 1000 mg), surfactant concentration, ratio of lipids and FA-DSPE (9:0.25 to 9:1), stirring speed (500 to 2000 rpm) and stirring time (30 to 75 min.) were identified as critical to give a product in nanorange and with required stability. All the factors were operated at four levels (1, 2, 3 and 4) which affect the mean particle size, PDI, zeta potential and drug entrapment efficiency. The concentration of drug, type of lipids, type of surfactant, stirring media, volume of stirring media, solvents were kept same for all the experiments. A total of 24 experiments were designed for further study.

2.5. Characterization of NLCs

2.5.1. Drug-Drug Compatibility

Drugs paclitaxel (5 mg) and gemcitabine hydrochloride (5 mg) were mixed with potassium bromide (100 mg) and compressed as pellets, for Fourier transforms Infrared (FTIR) Spectroscopic analysis to take spectra (Bruker Tensor-37, FTIR).

2.5.2. Particle size, poly-dispersity index (PDI), and zeta potential

Malvern zetasizer (Malvern Inc., Malvern, UK) was used for the estimation of particle size, PDI, and zeta potential. The diluted suspension of NLCs in phosphate buffer pH 7.4 was used for the measurement of size and PDI, while for zeta potential measurement; undiluted samples in de-ionized sterile water at 25° were used. All the measurement were recorded in triplicate.

2.5.3. Transmission electron microscopy (TEM)

Matrix structure and particle diameter of NLCs were visualized by transmission electron microscope (Hitachi, H-700 Transmission electron microscope, Japan). A drop of the formulation was placed on a carbon-coated copper grid surface. Beforehand the film dried, the film was negatively stained with 1% phosphotungstic acid immediately [14]. After one minute, excess fluid was removed and the grid was allowed to air dry exhaustively and formulations were observed under a TEM and photomicrographs were taken at appropriate magnification.

2.5.4. Scanning electron microscopy (SEM)

Shape and Surface morphology were determined by scanning electron microscopes (JEOL JSM-6700F). The samples for SEM were prepared by lightly sprinkling the NLCs powder on an adhesive tape, which was stuck on an aluminum stub. The stubs were then coated with gold to a thickness of about 300Å by using a sputter coater. All samples were examined under a scanning electron microscope at an acceleration voltage of 20kV, and photomicrographs were taken at suitable magnifications.

2.6. Percent Entrapment Efficiency (%EE)

The entrapment efficiency (EE) of GMP and PTX were determined using an ultrafiltration method for separating the non-entrapped drug from NLCs [15]. Briefly, 500 µL of GEM-PTX-NLCs and FA-conjugated GEM-PTX-NLCs were placed in an ultrafiltration tube (HITACHI himac CP 100MX) fitted with a filter membrane (molecular weight cutoff: 10 kDa). Free drugs in the underlying solution were collected by centrifugation at 8000 rpm for 15 min using a high-speed refrigerated centrifuge (3-18 K; SIGMA Laborzentrifugen GmbH, Osterode, Germany). The drug content of GEM and PTX in the ultrafiltrate (C_{free}) was determined simultaneously by high-performance liquid chromatography (HPLC) on a ZORBAX SB-C18 column (250 mm × 4.6 mm, 5 µm; Agilent Technologies, USA) at 268 nm. The mobile phase was 0.06 M ammonium acetate solution (pH 5.7, adjusted using glacial acetic acid)-acetonitrile. A gradient elution was used with a flow rate of 1.0 mL/min, where firstly 5% organic solvents (acetonitrile containing ammonium acetate solution) were held for 7 min, then amplified linearly to 70% over 10 min, where they were held for another 8 min and, finally, reduced linearly to 5% over 10 min, where they were held until the end of a 5 min run. The column temperature was retained at 25°C, and the injection volume was 10µL. Then, 0.5 mL of suspension was diluted with 2.0 mL of a mixture of tetrahydrofuran and 1 M HCl (70/30 v/v) solution, to determine the total drug concentration (C_{total}) by HPLC. The EE% was calculated using the following Equation:

$$\% EE = \{(C_{total} - C_{free}) / C_{total}\} \times 100$$

2.7. In vitro drug release behavior

The release behavior of GEM and PTX from NLC were assessed in phosphate-buffered saline (PBS) by the dialysis method [16, 17]. Briefly, the NLC were suspended in 5mL of the PBS pH7.4: methanol (7:3) and PBS pH4.0: methanol (7:3) release medium and transferred into a

dialysis bag (MWCO 3500 Da). The release investigation was started by placing the dialysis bag into 45 mL of release medium with constant shaking at 100 rpm at 37°C. At a scheduled time, 4mL of the incubated solution was withdrawn and substituted with equal volume of fresh release medium. The amount of GEM and PTX contents in the samples were measured by HPLC mentioned in the above section.

2.8. Stability Studies

GEM-PTX-NLCs) and FA-conjugated GEM-PTX-NLCs) were the two optimized formulations, subjected to stability testing under storage condition at $5\pm 3^\circ\text{C}$ and $25\pm 2^\circ\text{C} / 60\pm 5\%$ RH as per International conference on harmonisation guideline Q1A(R2) 2.2.7.4. Both formulations were stored in screw capped, amber colored small glass bottles at $5\pm 3^\circ\text{C}$ and $25\pm 2^\circ\text{C} / 60\pm 5\%$ RH. Analysis of the samples was made for particle size and residual drug content after a period of 15, 30, 45 and 60 days.

2.9. Statistical analysis

All the results were reported as mean \pm SD (standard

deviation). By applying one-way ANOVA, the statistical significance was determined. The differences between experimental groups when the p value was less than 0.05 ($p < 0.05$) were considered significant.

3. RESULTS AND DISCUSSION

3.1. Folate-DSPE Conjugates

The final conjugates were synthesized by forming an amide bond between the carboxylic group of folic acid and the amine group of DSPE. Folate-DSPE conjugates were characterized by FTIR and ^1H NMR spectroscopy (fig. 1a, b). A typical signal of amide stretch ($\text{C}=\text{O}$) absorption band at 1603 cm^{-1} and amide banding ($\text{N}-\text{H}$) at 1511 cm^{-1} , confirmed the synthesis of NHS folate-DSPE conjugates (fig. 1a). Conjugates were further characterized by ^1H NMR, and the characteristic peaks of methyl protons of DSPE are recorded at about 3-3.6 ppm. The proton peaks at 5-6 ppm confirmed the formation of amide bond between the carboxylic group of folic acid and the amine group of DSPE and the characteristic peaks of folic acid ring-associated protons recorded at about 8-9 ppm; ^1H NMR confirmed the synthesis of NHS folate DSPE conjugates (fig. 1b).

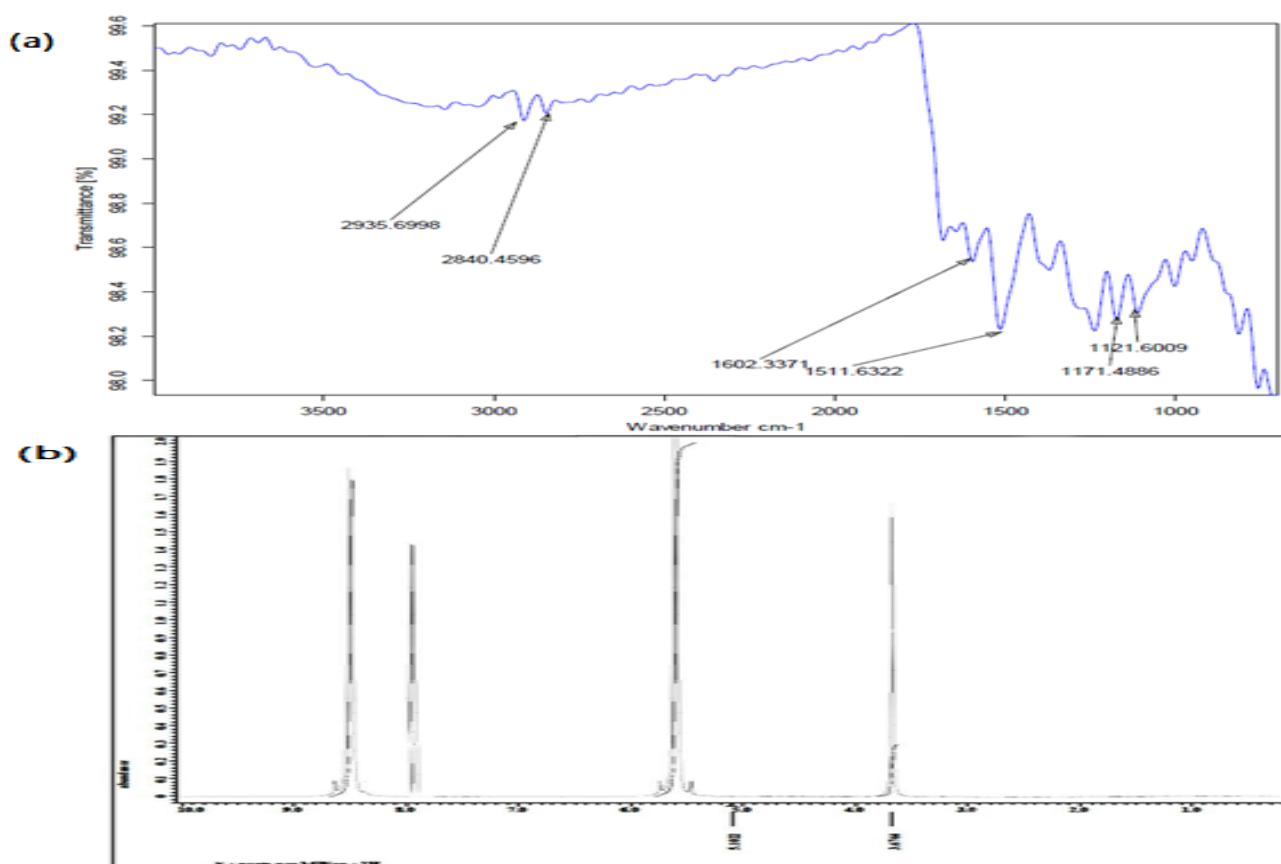
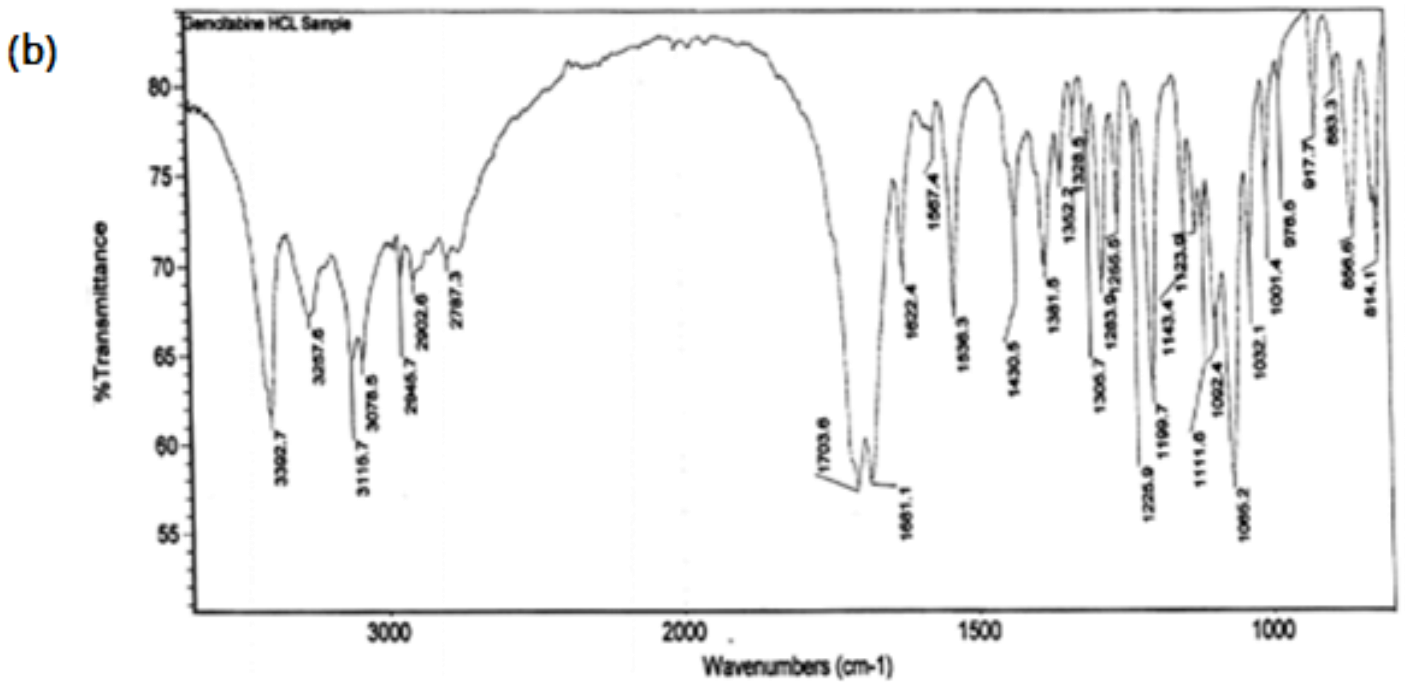
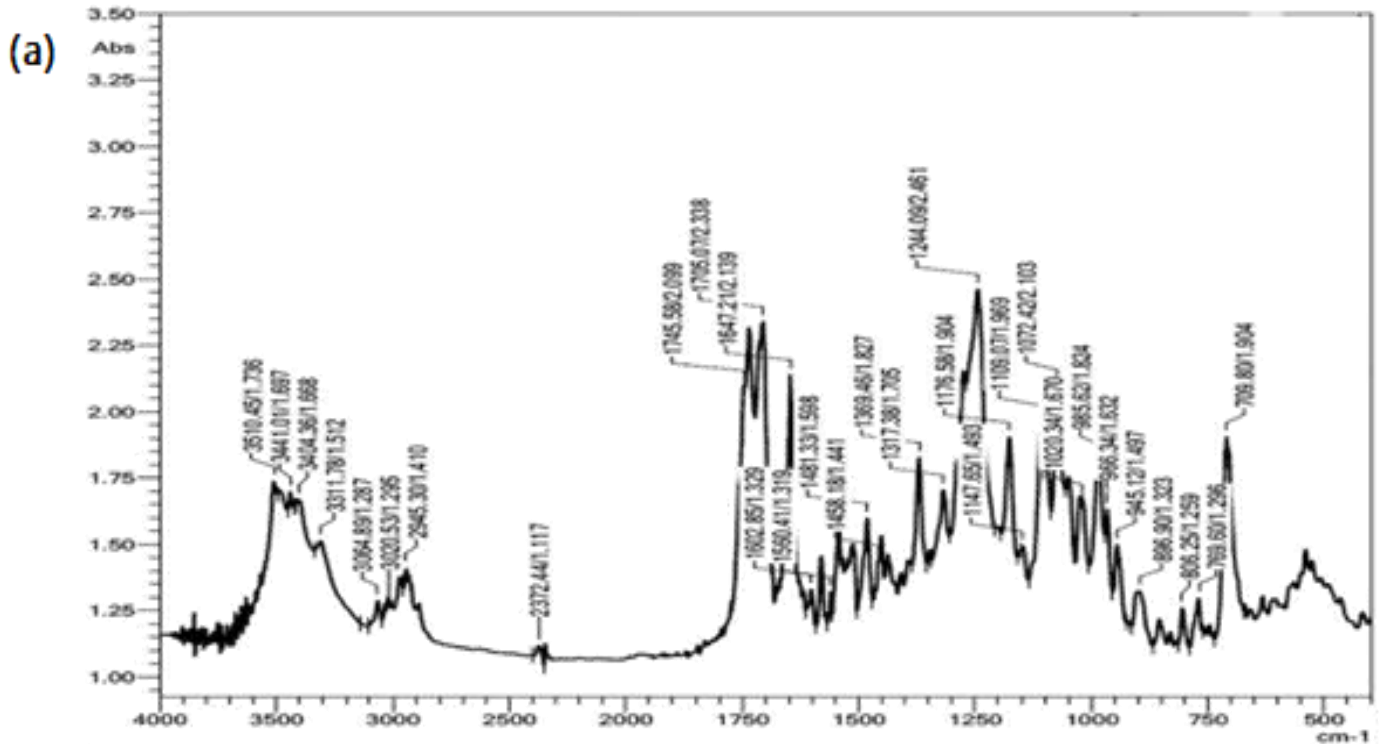


Fig. 1: a) FTIR and b) ^1H NMR spectroscopy of NHS-Folate DSPE conjugates

3.2. Drug-Drug Compatibility

Fourier-transform infrared spectroscopic interpretation reveals the specific signal of (C-O) stretch of secondary alcohol at 1143 cm^{-1} , typical signal of out-of-plane O-H band at 650 cm^{-1} and characteristics absorption bands of C=O stretch of ester and acid at 1735 and 1710 cm^{-1} respectively, confirmed the presence of paclitaxel (fig. 2a). Similarly, characteristic peaks of amine bands at

1680 cm^{-1} and characteristic peak of ureido group at 1721 cm^{-1} with 3393 cm^{-1} for stretching vibration of (NH_2) confirmed the presence of gemcitabine hydrochloride (fig. 2b). Fig. 2c shows both the standard spectra of paclitaxel, gemcitabine hydrochloride, and mixture of paclitaxel and gemcitabine hydrochloride which also confirm the compatibility of the drugs with no interaction between the drugs or excipients.



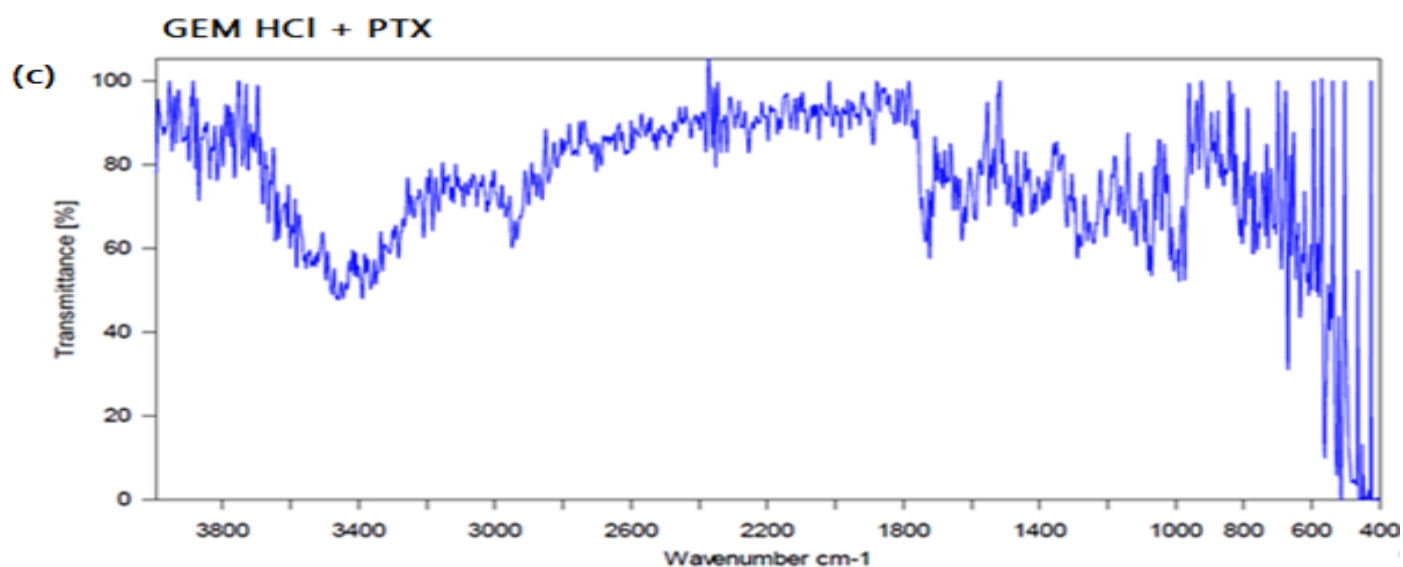


Fig. 2: FTIR of a) Paclitaxel b) Gemcitabine hydrochloride c) Gemcitabine hydrochloride + Paclitaxel (mixture)

3.3. Preparation of NLCs

Preparation of FA-conjugated GEM-PTX-NLCs was carried out employing emulsion-evaporation method. The prepared NLCs formulation was optimized for various parameters like liquid lipid (Soybean Phosphatidylcholine) concentration, solid lipid (Stearic acid) content, surfactant (cetrimide) concentration, lipid: FA-DSPE ratio, stirring speed and stirring time to obtain nano sized NLCs with maximum drug entrapment. Lipid employed in the production of NLCs was first subjected to optimization by varying the lipid concentration from 250-1000 mg, and further optimizing stearic acid content from 250-1000 mg. Optimized particle size and polydispersity index (PDI) of NLCs were obtained with 50% each of the lipids (fig. 3a, b). It could be clearly observed that the average size of the NLCs decreased with the increase of liquid lipid amount. For both solid fats and liquid oils, a high proportion of long chain triacylglycerols contributed to large NLC particles. On the other hand, the size of NLC particles decreased with the increase of liquid oil for the same kind of bulk lipids. This was due to the fact that liquid oil could be easily dispersed into the aqueous phase and contributed to smaller particles [18]. The particle size was found to be decreased upon increasing the concentration of Cetrimide (fig. 4). This might be due to decrease in the surface tension between organic phase and aqueous phase, which is ultimately seen to allow formation of nano range particles. Particles of optimum size with maximum drug entrapment were

obtained at 0.5% surfactant concentration. However, on further increasing surfactant concentration, the particle size decreased because of formation of micelles and the %EE also decreased because of the leaching out the drug. Further, lipid: FA-DSPE ratio 9:1 was considered on the basis of optimized particle size, PDI and %EE (fig. 5a, b). Particle size decreased on increasing the stirring speed but after a period, particle size was increased (fig. 6). On varying the stirring time, particle size showed variation but drug entrapment decreased as shown in fig. 7 [19]. The obtained FA-conjugated GEM-PTX-NLCs formulations existed as a milky emulsion with an off-white to pale-yellowish color.

3.4. Characterization of NLCs

Zeta potential, PDI and particle size of NLCs were characterized and summarized in table 1. The results showed that particle size of GEM-PTX-NLCs and FA-conjugated GEM-PTX-NLCs were found to be 122.16 ± 3.75 and 134.62 ± 4.11 nm respectively without significant difference. The average NLCs size reported for different formulations had an average size less than 200 nm (107 to 195 nm) with a narrow PDI which was within an acceptable range for intravenous injection [20]. Fig. 8a and b represent the size distribution curve of GEM-PTX-NLCs and FA-conjugated GEM-PTX-NLCs, respectively. The Zeta potential was invariably positive for all NLCs after preparation. Due to the presence of cationic surfactants,

NLCs have positive zeta potential which facilitates their efficient cellular interaction and uptake through endocytosis. It could have proceeded through bio cell-associated negative charge, liable to interacting with cationic charge bearing composites, resulting in cell

penetration and subsequent internalization [19]. The cationic charge on NLCs may provide endosomal destabilization resulting in burst release of both drugs (gemcitabine and paclitaxel) in the cytosol.

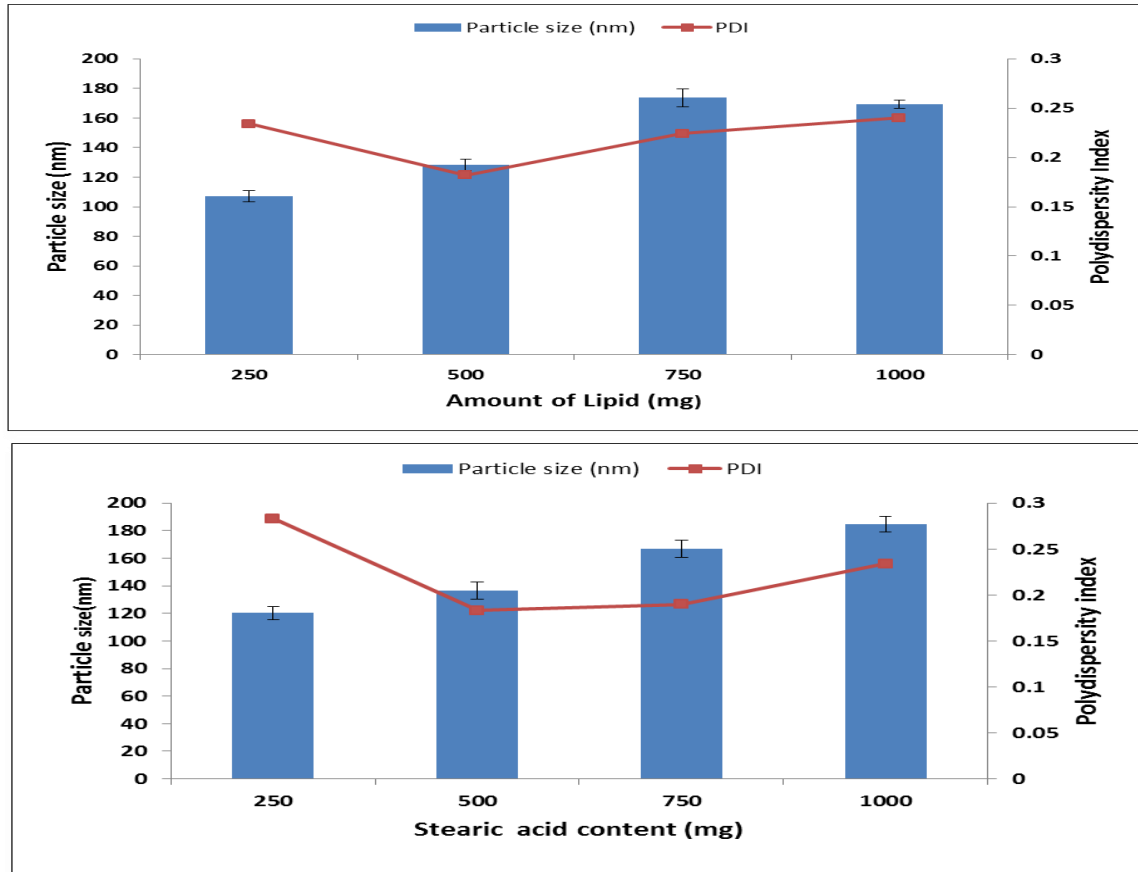


Fig. 3: Optimization of Lipid content a) liquid lipid b) solid lipid, with regard to particle size (nm) and polydispersity index

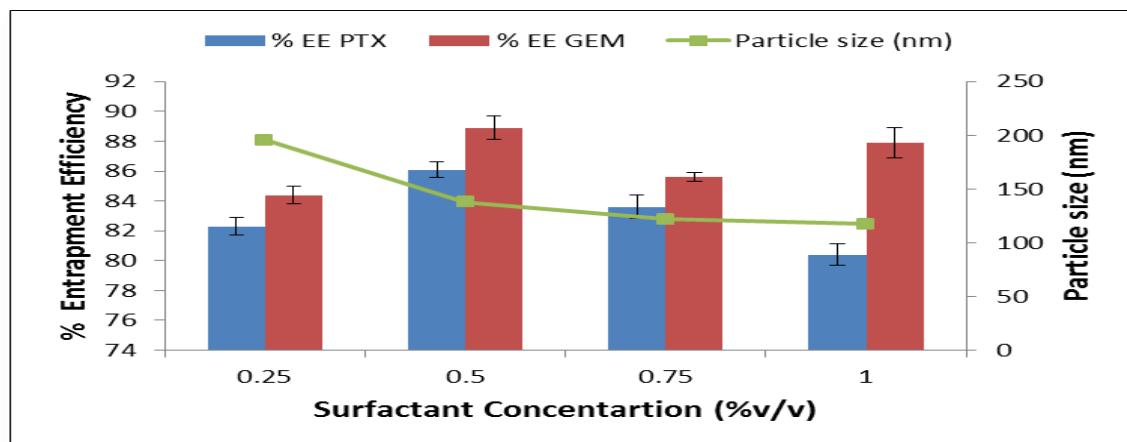
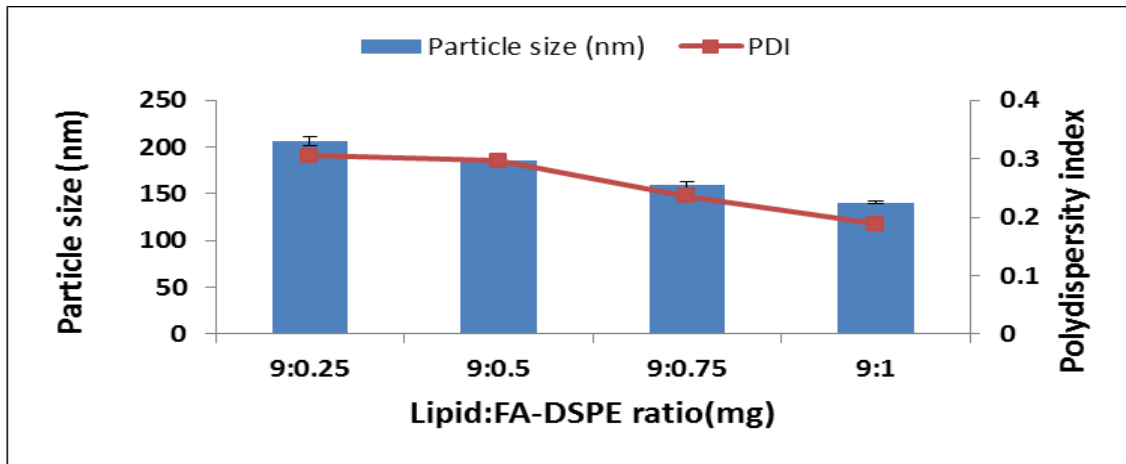


Fig. 4: Optimization of surfactant concentration (%w/v) with regard to particle size (nm) & % drug entrapment efficiency of PTX & GEM HCl

a)



b)

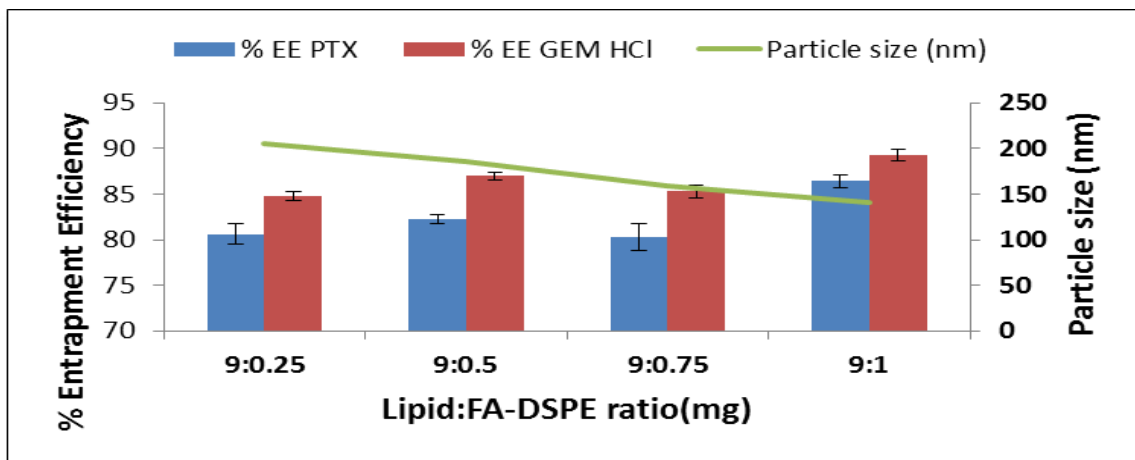


Fig. 5: Optimization of lipid : FA-DSPE (mg) with regard to a) particle size(nm) and polydispersity index b) particle size (nm) and % drug entrapment efficiency of PTX and GEM

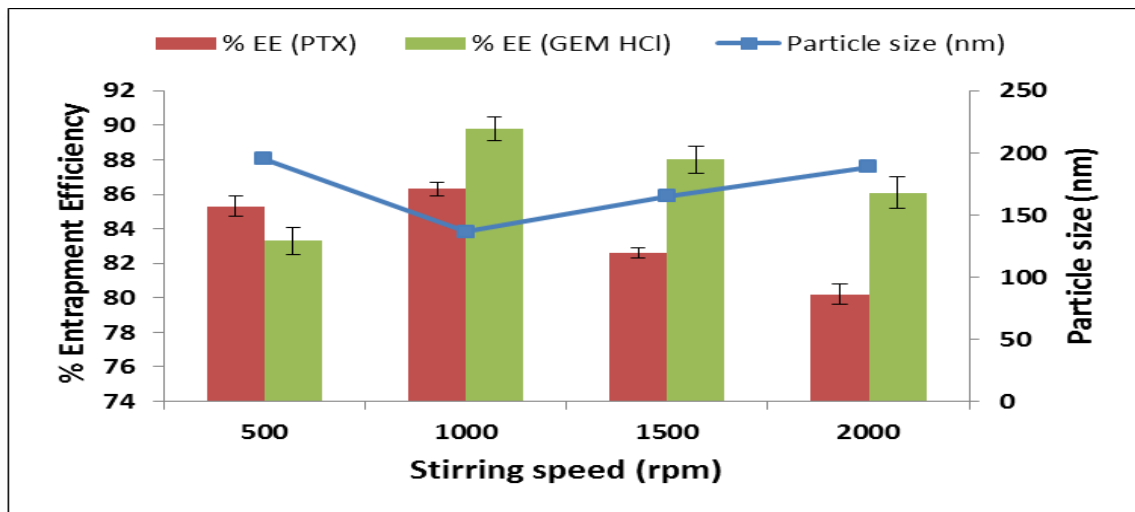


Fig. 6: Optimization of stirring speed (rpm) with regard to particle size (nm) & % drug entrapment efficiency of PTX & GEM

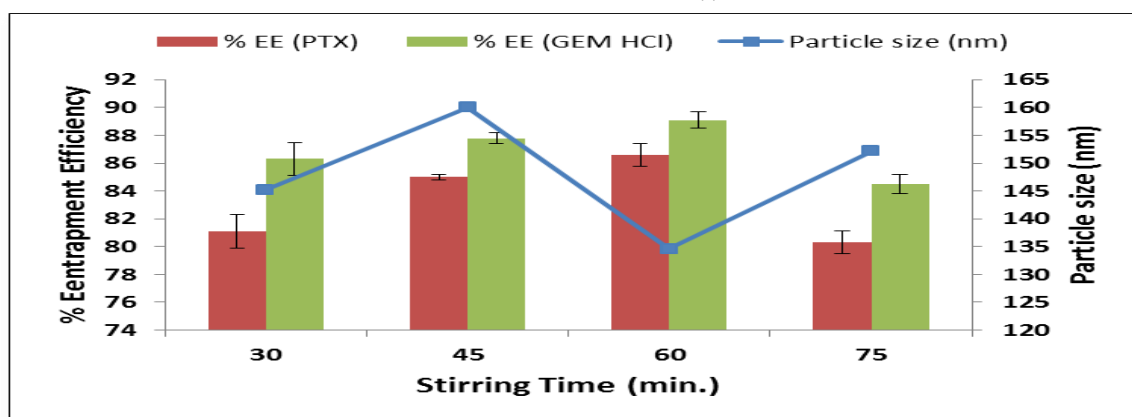


Fig. 7: Optimization of stirring time (min.) with regard to particle size (nm) & % drug entrapment efficiency of PTX & GEM

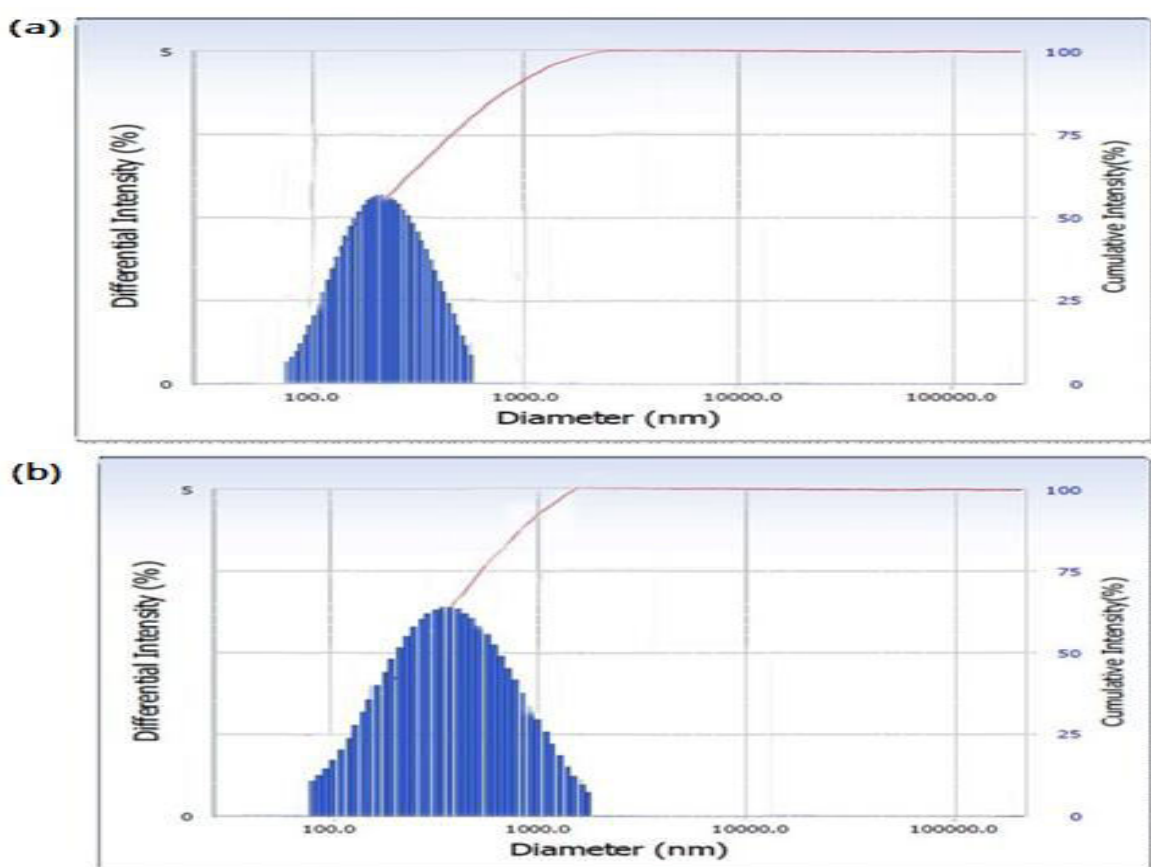


Fig. 8: Size distribution curve of a) GEM-PTX-NLCs b) FA-conjugated GEM-PTX-NLCs

Table 1: Optimized formulation variable

Formulation	Soybean PC content (mg)	Stearic acid content (mg)	Cetrimide Concentration (% w/v)	Lipid: FA-DSPE ratio	Stirring Speed (rpm)	Stirring Time (min.)	Particle Size (nm)	PDI	Zeta Potential (mV)
GEM-PTX-NLCs	500	500	0.5	9:1	1000	60	122.16±3.75	0.142±0.09	+16.6±0.8
FA-conjugated GEM-PTX-NLCs	500	500	0.5	9:1	1000	60	134.62±4.11	0.189±0.05	+28.4±0.6

3.4.1. Transmission Electron Microscopy (TEM)

Optimized GEM-PTX-NLCs and FA-conjugated GEM-PTX-NLCs were observed under TEM. TEM image of dried suspension of GEM-PTX-NLCs and FA-conjugated GEM-PTX-NLCs were smooth and nearly spherical. It was evident from TEM studies that the developed NLCs were of nanometric size range. GEM-PTX-NLCs and FA-conjugated GEM-PTX-NLCs were viewed under a transmission electron microscope, and photomicrographs were represented in fig. 9a, b.

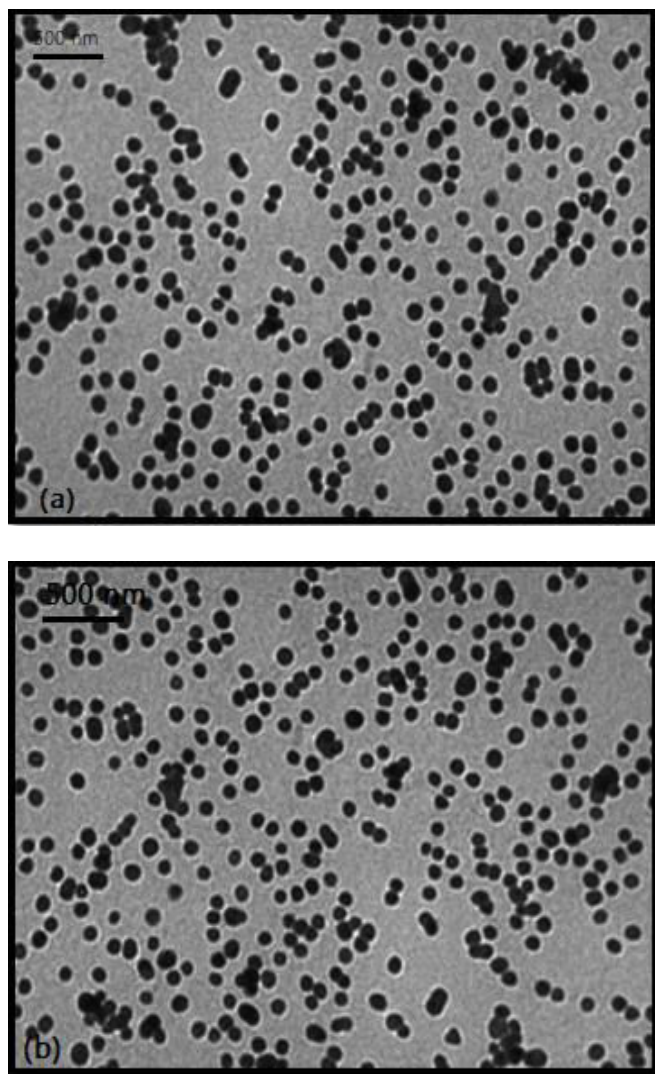


Fig. 9: TEM photomicrograph of NLCs a) GEM-PTX-NLCs b) FA-conjugated GEM-PTX-NLCs

3.4.2. SEM studies

Micrographs obtained by SEM confirmed the globular nature and spherical shape of nanoparticles. Fig. 10a and Fig. 10b depict the morphology of GEM-PTX-NLCs and FA-conjugated GEM-PTX-NLCs respectively.

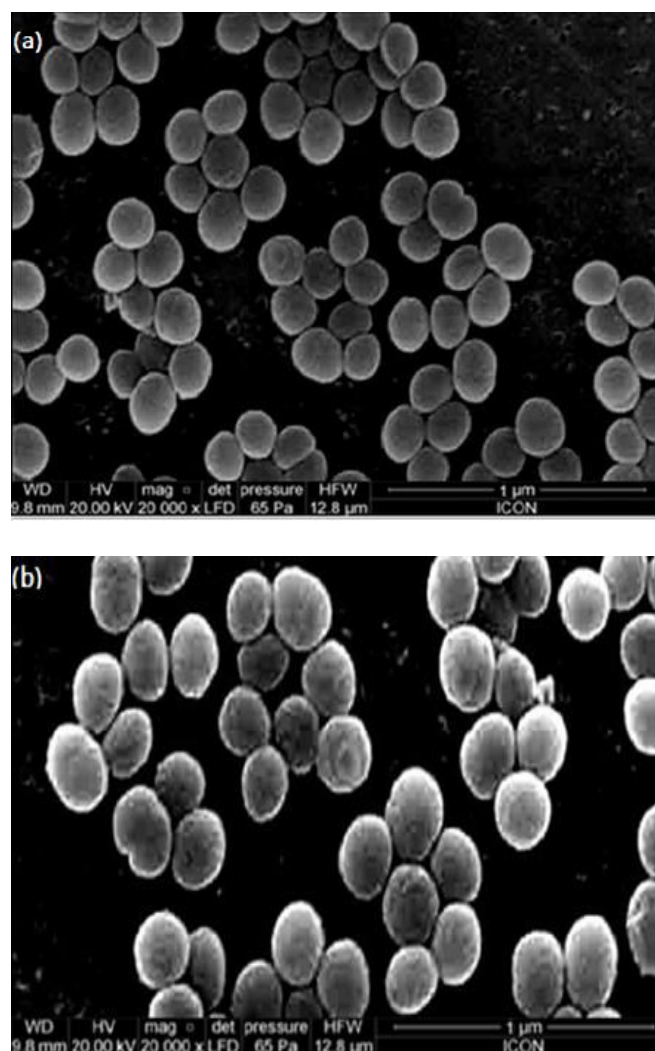


Fig. 10: SEM photomicrograph of a) GEM-PTX-NLCs b) FA-conjugated GEM-PTX-NLCs

3.5. Percent Entrapment efficiency (%EE)

%EE of GEM and PTX were calculated to be $87.4 \pm 0.8\%$ and $82.7 \pm 0.6\%$ respectively in the GEM-PTX-NLCs while in the FA-conjugated-GEM-PTX-NLCs it was $89.1 \pm 0.6\%$ and $86.6 \pm 0.8\%$ respectively. This variation may be due Particle size of GEM-PTX-NLCs formulation was smaller than FA-conjugated GEM-PTX-NLCs. The drug entrapment efficiency of GEM-PTX-NLCs was less than that of FA-conjugated-GEM-PTX-NLCs. EE % significantly affects the release of the drug from NLCs as higher encapsulation alters the concentration gradient and rate of drug release [21].

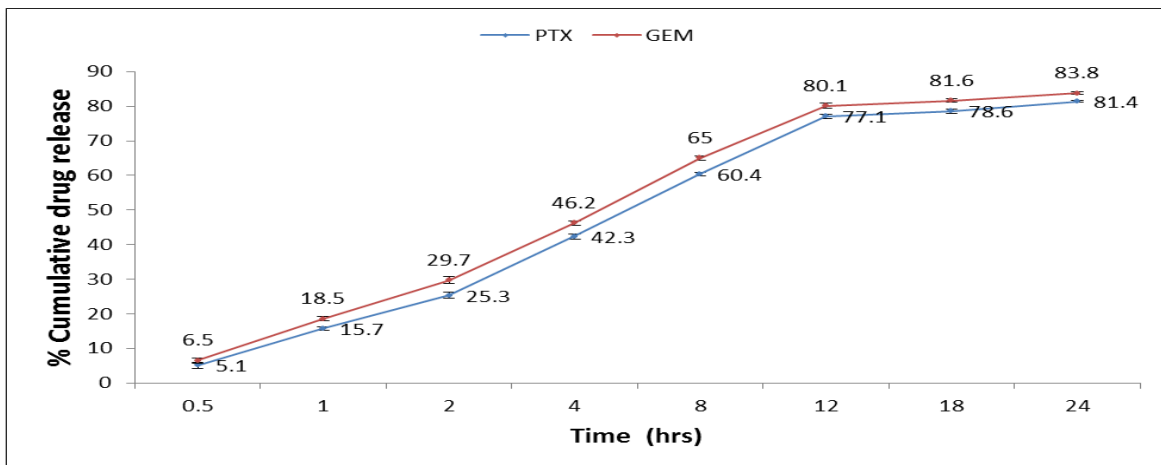
3.6. In vitro drug release study

To examine the pH dependence of drug release with respect to time, release of GEM and PTX from NLCs and FA-NLCs were quantified by high-performance

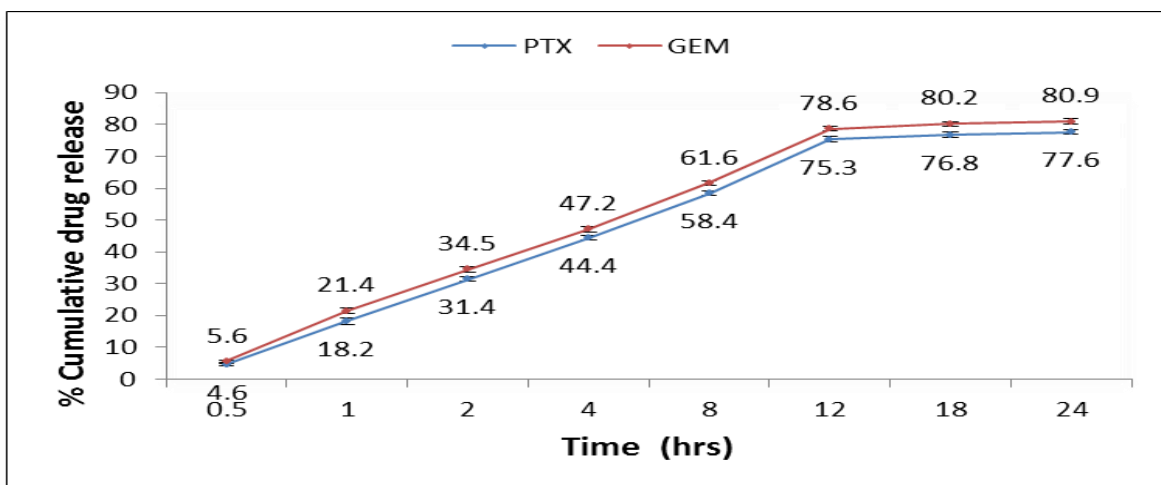
liquid chromatography in PBS at pH 7.4 and PBS at pH 4.0 containing methanol (7:3) to mimic the normal extracellular environment and reductive cytosolic environment respectively. Formulation GEM-PTX-NLCs showed cumulative drug release 80.1 ± 0.72 and $77.1 \pm 0.62\%$ for gemcitabine and paclitaxel respectively in 12 h in PBS pH 7.4: methanol (7:3). The release pattern is graphically shown in fig. 11a, while folic acid-conjugated GEM-PTX loaded NLCs showed 78.6 ± 0.93 and $75.3 \pm 0.7\%$ cumulative release of gemcitabine and paclitaxel respectively in 12 h in PBS pH 7.4: methanol (7:3) as shown graphically in fig. 11b, indicating relatively slower release of drugs in case of folate-conjugated NLCs compared to unconjugated NLCs at pH 7.4. Furthermore, the cumulative drug release was also studied at pH 4 as well, and the formulations of GEM-PTX-NLCs showed cumulative drug release 89.3 ± 0.93 and $84.5 \pm 0.83\%$ of gemcitabine and paclitaxel, respectively, in 12 h in PBS pH 4.0:

methanol (7:3) as shown graphically in fig. 11c, while folic acid-conjugated GEM-PTX-NLCs showed cumulative drug release 85.5 ± 0.75 and $82.2 \pm 0.72\%$ of gemcitabine and paclitaxel, respectively, in 12 h in PBS pH 4.0: methanol (7:3) as shown graphically in fig. 11d. Release patterns at different pH values revealed that GEM released more quickly than PTX at an early time point. This might be due to GEM being extensively smaller than PTX, which can cause less steric hindrance toward hydrolysis [22]. The results suggested relatively slower release of drugs in case of conjugated NLCs as compared to unconjugated NLCs because NLCs conjugated with folic acid mitigated the release of drug by constituting a secondary barrier. Nevertheless, the drug(s) release in PBS at pH 4 was faster as compared to pH 7.4, suggesting a pH-modulated drug(s) release, which would be facilitated by the acidic bio environment of tumor or in the endosomes especially in the case of targeted drug delivery.

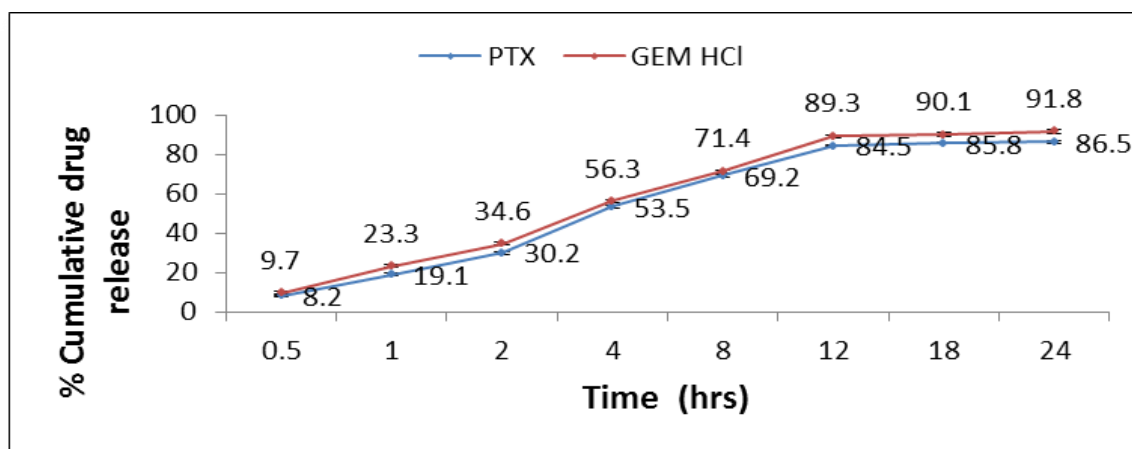
a)



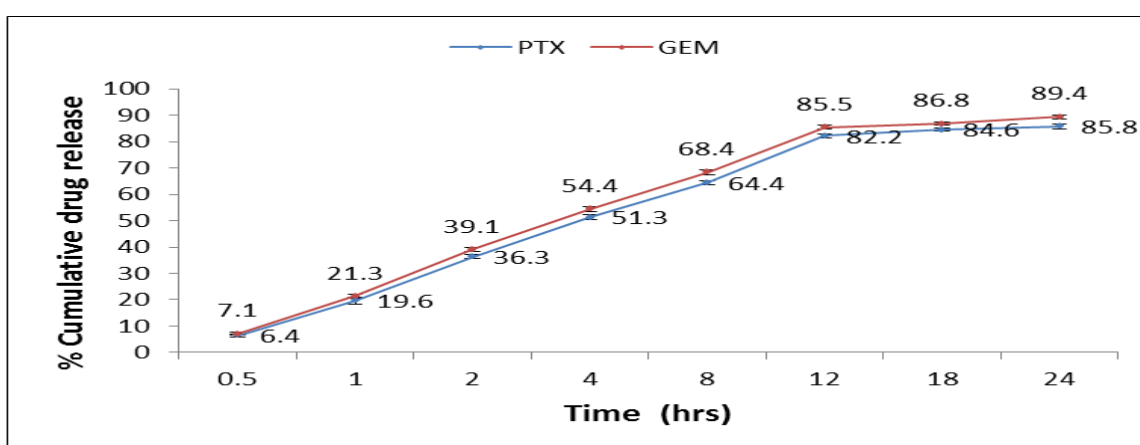
b)



c)



d)



a) GEM-PTX-NLCs in PBS pH 7.4: methanol (7:3) b) FA-conjugated GEM-PTX-NLCs in PBS pH 7.4: methanol (7:3) c) GEM-PTX-NLCs in PBS pH 4.0: methanol (7:3) d) FA-conjugated GEM-PTX-NLCs in PBS pH 4.0: methanol (7:3).

Fig. 11: In vitro percent cumulative drug release profile of PTX and GEM from NLCs

3.7. Stability studies

The results for stability of GEM-PTX-NLCs and FA-conjugated GEM-PTX-NLCs were found to be similar in appearance (yellowish oily liquid) at the end of stability studies at 15, 30, 45, and 60 days as on day 0. NLCs were found to form a uniform emulsion when reconstituted with water. No signs of lump formation and drug precipitation were noticed. Furthermore, mean particle size and residual drug content were observed at all conditions of stability. A little change in average particle size was observed on storage even after 60 days in both cases which was lesser in case of the formulation stored at $5\pm 3^{\circ}\text{C}$ than those stored at $25\pm 2^{\circ}\text{C}/60\pm 5\%$ RH. This might be due to the fusion of particles, which increased with increase in temperature (fig. 12a, b). Percent residual drug content results revealed significant loss of drug in case of

formulation stored at $25\pm 2^{\circ}\text{C}/60\pm 5\%$ RH as compared to little loss of drug with formulation stored at $5\pm 3^{\circ}\text{C}$. Nearly similar results were obtained for folate conjugated nanostructured lipid carriers when analyzed separately. It may be concluded that formulation stored at $5\pm 3^{\circ}\text{C}$ was quite stable as very less drug was released on storage for 60 days as compared to the product stored at $25\pm 2^{\circ}\text{C}/60\pm 5\%$ RH. The more drug loss at $25\pm 2^{\circ}\text{C}/60\pm 5\%$ RH could be due to the leakage of drugs from NLCs as shown in fig. 13a, b [23]. The stability testing data indicated that nanostructured lipid carrier formulations stored at $5^{\circ}\text{C}\pm 3^{\circ}\text{C}$ were more stable than those stored at $25\pm 2^{\circ}\text{C}/60\pm 5\%$ RH. Hence $5\pm 3^{\circ}\text{C}$ may be suggested as the storage temperature for NLCs formulations for their better stability.

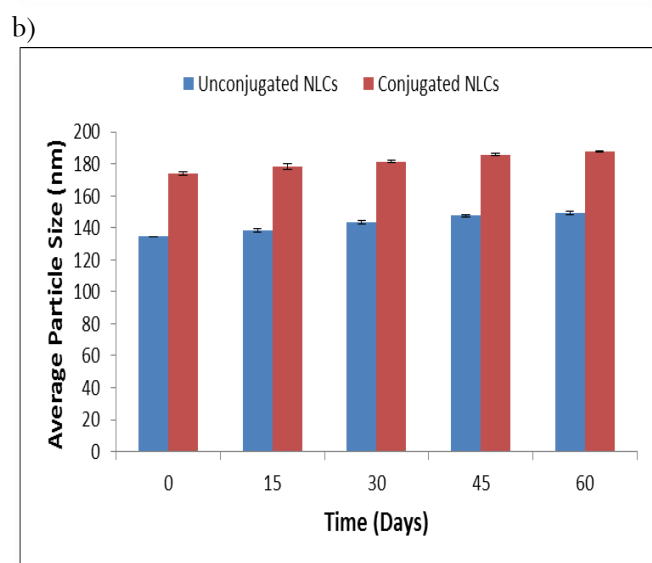
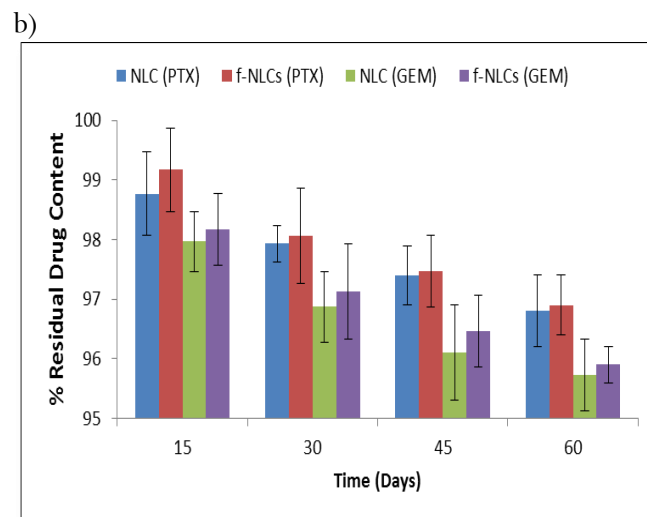
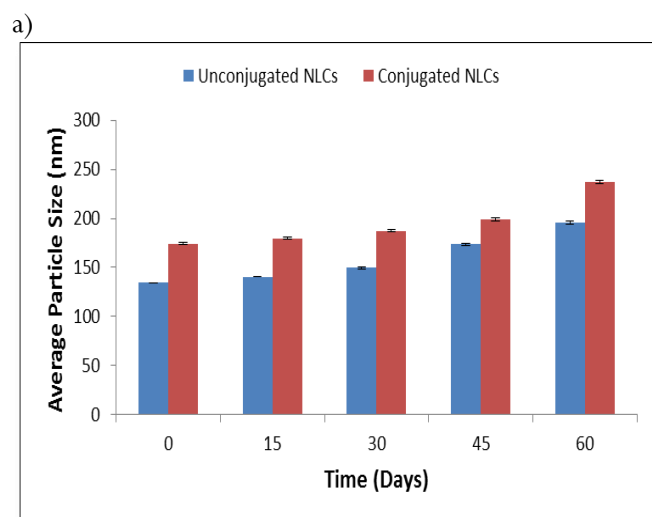


Fig. 12: Effect of storage temperature on the particle size at a) $5\pm 3^{\circ}\text{C}$ b) $25\pm 2^{\circ}\text{C} / 60\pm 5\% \text{RH}$

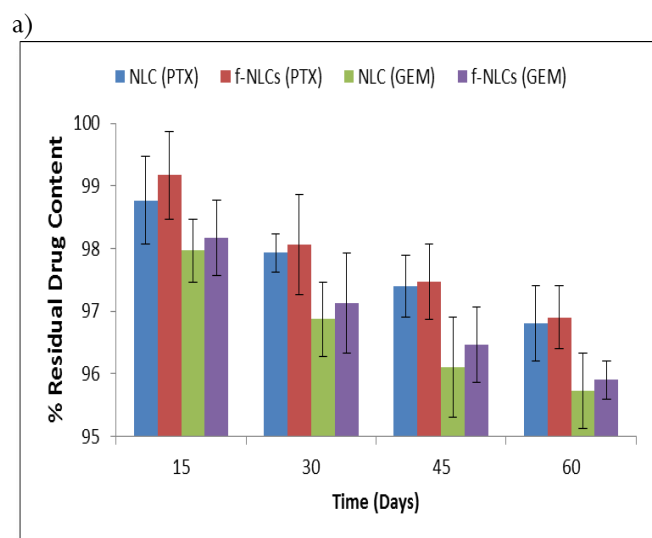


Fig. 13: Effect of storage temperature on drug content of NLCs at a) $5\pm 3^{\circ}\text{C}$ b) $25\pm 2^{\circ}\text{C} / 60\pm 5\% \text{RH}$

4. CONCLUSION

Nanostructure lipid carrier system offers a promising dosage form for combination cancer therapy by concurrently loading two or more kinds of chemotherapeutics. Herein, ligand/pH dual responsive nanocarrier folic acid-conjugated GEM-PTX NLCs was prepared and characterized. Particle size less than 200 nm with low polydispersity index was successfully achieved for delivery of dose to the circulation. To load a proper amount of drug in NLCs, entrapment efficiency above 60% was achieved. This dual drug loaded NLCs exhibited efficient drug release on PBS pH 4.0 for 12 h. Refrigerated storage condition was found to be excellent stability of formulation FA-conjugated-GEM-PTX-NLCs. This study revealed that formulation FA-conjugated-GEM-PTX-NLCs has potential for the management of cancer through parenteral route.

Declaration of interest

The authors declare no conflict of interest.

5. ACKNOWLEDGEMENTS

The authors would like to thank RKDF University, Bhopal for providing excellent infrastructure facility for research work.

6. REFERENCES

- Muller RH, Mehnert W, Lucks JS, Schwarz C, et al. *Eur J Pharm Biopharm*, 1995; **41**:62-69.
- Muller RH, Radtke M, Wissing SA. *Int J Pharm*, 2002; **242**:121-128.

3. Muller RH, Mader K, Gohla S. *J Pharm Biopharm*, 2000; **50**:161-177.
4. Salvi VR, Pawar P. *J Drug Del Sci Tech*, 2019; **51**:255-267.
5. Gupta A, Kaur CD, Saraf S, et al. *J Recept Sig Transd*, 2017; **37(3)**:314-323.
6. Comparetti EJ, Lins PMP, Quitiba JVB, Zucolotto V. *Materials Advances*, 2020; **1**:1775-1787.
7. Staff RH, Landfester K, Crespy D. *Adv Polym Sci*, 2013; **262**:329-344.
8. Naseri N, Valizadeh H, Zakeri-Milani P. *Adv Pharm Bull*, 2015; **5**:305-313.
9. Gonzalez-Mira E, Egea MA, Souto EB, et al. *Nanotechnology*, 2011; **22**:045101.
10. Fang CL, Al-Suwayeh S, Fang JY. *Recent Pat Nanotechnol*, 2013; **7**:41-55.
11. Sue Lee C, Koo J. *Expert Opin Pharmacother*, 2005; **6**:1725-1734.
12. Lee RJ, Low PS. *Biochim et Biophysica Acta*, 1995; **1233**: 134-144.
13. Di H, Wu H, Gao Y, et al. *Drug Dev Ind Pharm*, 2016; **42**:2038-2043.
14. Hu FQ, Jiang SP, Du YZ, et al. *Int J Pharm*, 2005; **45**:167-173.
15. Zhang J, Zhang P, Zou Q, et al. *Molecules*, 2018; **23**:2906.
16. Lin T, Fang Q, Peng D, et al. *Drug Deliv*, 2013; **20**:277-284.
17. Lv S, Tang Z, Li M, et al. *Biomaterials*, 2014; **35**: 6118-6129.
18. Zheng M, Falkeborg M, Zheng Y, et al. *Coll Sur Physico Eng Asp*, 2013; **430**:76-84.
19. Raikwar S, Vyas S, Sharma R, et al. *AAPS Pharm Sci Tech*, 2018; **19(8)**:3839-3849.
20. Chinsriwongkul A, Chareanputtakhun P, Ngawhirunpat T, et al. *AAPS Pharm Sci Tech*, 2011; **13(1)**:150-158.
21. Mohamed H, Shifaa MA, Leena K, Gorka O. *Pharmaceutics*, 2020; **12**:288.
22. Liang Y, Tian B, Zhang J, et al. *Int J Nanomed*, 2017; **12**:1699-1715.
23. Prachi BK, Swapnil ST, Vandana BP. *Int J Pharm*, 2020; **577**:119082.